Proc. of the 9th Intl. Conf. of Asian Society for Precision Engg. and Nanotechnology (ASPEN 2022)
15–18 November 2022, Singapore. Edited by Nai Mui Ling Sharon and A. Senthil Kumar
doi://10.3850/978-981-18-6021-8_OR-02-0212

Investigation on the Process Parameters of an Automated Wall Grinding Robotic System

Landong Martua[1], and Mustafa Shabbir Kurbanhusen[1,#]
1 Engineering Cluster, Singapore Institute of Technology, 10 Dover Drive, 138683, Singapore
Corresponding Author / Email: Mustafa.Shabbir@Singaporetech.edu.sg, TEL: +65 6592 2190

KEYWORDS: Cable-driven robots, Concrete Wall Grinding, Design of Experiments

In the construction industry, handheld grinders are typically used to grind-off various concrete wall surface defects such as cement drips, bulges and rough patches, prior to the skimming and painting processes. Grinding results in a very dusty environment, posing health and safety risks to the construction workers. There are solutions which aim to alleviate the strenuous polishing/grinding work through the use of supporting structures, and incorporating a vacuum system with the aim of minimizing the dust produced. However, the human worker is still vital to the operations. These concerns, coupled with a shortage of construction workers led to the need of an automated wall grinding robotic system to lower the risk of accidents and streamline construction processes, thereby saving time and cost. This paper first presents the design of a three degrees-of-freedom planar, parallel robot, based on the cable-driven parallel mechanism design and commercially available scaffolding structures with trolley wheels to create a reconfigurable wall polishing/grinding robotic system. One of the key enablers in transitioning from manual to automated grinding is the understanding of the appropriate grinding process parameters, in order to obtain an acceptable surface finishing. This is followed by the investigation of the key grinding process parameters, through the use of Design-of experiments to identify relevant and dominant parameters that are suitable for automated wall grinding. The identified grinding process parameters consisted of the normal grinding force, the grinding rotational speed and the type of grinding media. Based on an experimental test-bed that facilitated in the grinding process, the preliminary results indicate that the grinding of common defects requires a normal grinding force of approximately 30N, with a grinding speed of 9000 rpm and using the single-row diamond cup wheel as the grinding media.

NOMENCLATURE

n = number of degree of freedoms (DOFs)
m = required number of cables
PPVC = Prefabricated Prefinished Volumetric Construction

1. Introduction

Current polishing/grinding method typically involves manual labor using a handheld grinding tool to grind off defects of the walls, which is time consuming and hazardous due to the dust particles that are created during polishing/grinding process. In addition, the current environmental and health crisis further worsened the manpower shortage issue. There are solutions which aim to alleviate the strenuous polishing/grinding work through the use of supporting structures, and incorporating a vacuum system with the aim of minimizing the dust produced. However, the human worker is still vital in the operations. There have also been semi-automated polishing/grinding solutions [1] which consists of a rotary machine with a large diameter grinding media.

Such system requires tracks on the floor to consistently traverse along the wall and polish/grind it. It still requires a human worker and the effort in laying tracks on the floor increases the operational costs. While some of the current solutions mitigate some of the hazards like the use of vacuum to minimize dusts, the use of supporting frames to ease the load from the worker, larger grinding media to hasten the polishing, these solutions still require a human worker to co-exist, which presents a gap to be addressed in times where manual labor is in short supply.

In the following sections, this paper will detail the design overview of the proposed automated wall grinding robotic system, including its kinematic model, followed by the experimental trials and the obtained results.

2. Design Overview of the Automated Wall Grinding Robotics System

The automated wall grinding robotics system consists of a set of cable winches, each winding/unwinding their own respective cable, which are all routed through a set of configurable cable attachment points and are attached to a common end-effector (EE), as shown in Fig. 1 Through the coordinated winding/unwinding of each cable, this will enable the end-effector to move in synchronized manner about a surface bounded by the locations of the cable attachment points and carry out the polishing/grinding tasks.

The cable winching unit consists of integrated motors that drives a winding drum via a timing belt and pulley transmission. The end-effector is also designed to incorporate existing handheld grinders and achieve a similar and more consistent polishing/grinding outcome, as compared to a human worker. This also minimizes the setup time and costs. The other feature of this system is its ability to modify the polishing/grinding force through the adjustment of the cable forces. This facilitates in fine tuning process parameters depending on the material of the surface to bel polished/grinded.

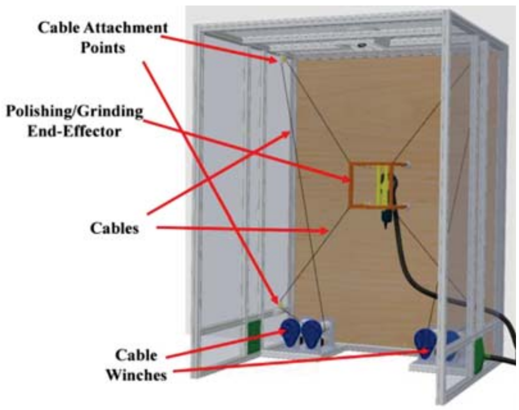

Fig. 1 Conceptual design of the cable-driven manipulation system for wall polishing and grinding

3. Kinematics model with Cable Extension compensation factor

A fully constrained Cable-Driven Parallel Robot (CPDR) with n number of degree of freedoms (DOFs) requires number of cables, $m=n+1$. If $m<n+1$ the CPDR is under-constrained and *if* $m>n+1$ the CPDR is redundantly constrained. A 2-DOFs planar translation require at least 3 cables to avoid slack and lose control because of the unilateral driving property of cables i.e., only able to exert tension [2] [3].

Fig. illustrate the structure of the 2 DOF planar translation CPDR where P_j (j=1, 2, 3, 4) are pulleys that connect j^{th} cables to the base frame, L_j represent lengths of the j^{th} cables and θ_j are the cable angles. Four cables are connected to the four corners of the EE. Changing the cable lengths will change the location of the EE, (x,y). The origin of the cartesian space is located at center of the pulley 1 (X_0, Y_0). Kinematics and statics modeling are derived from geometric relations between base frame, cables, and EE.

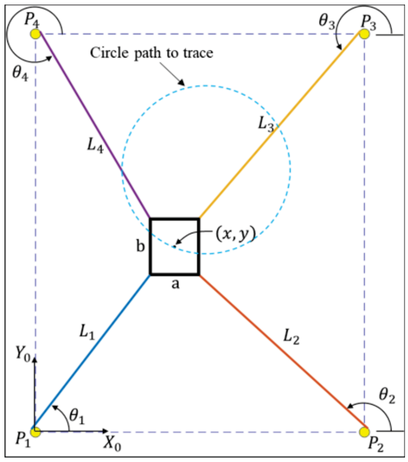

Fig. 2 CPDR Kinematics diagram

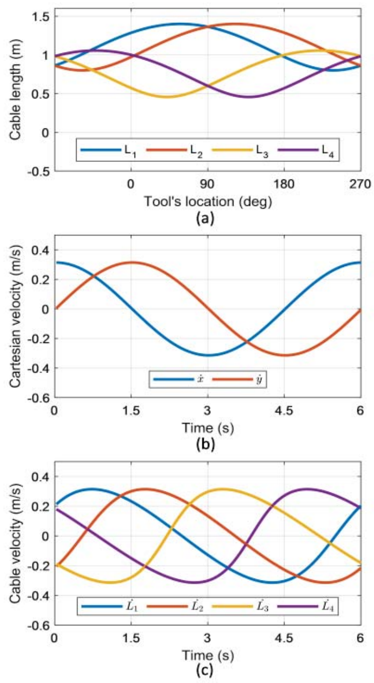

Fig. 3 (a) Required cable lengths to perform a circular path tracing (r=0.3m), (b) EE cartesian velocity, (c) EE joint velocity.

The kinematics model is simulated to command the end-effector (EE) frame to trace a pre-defined circle path with a radius 0.3m on the wall surface as shown in Fig. . The dimension of the model follows the detailed dimension of the prototype. Start and end positions of the EE is at 270°. Results are plotted with respect to this position.

Fig. (a) plotted all the required cable lengths to perform the circular path tracing. It can be observed that cable 1 and cable 2 as well as cable 3 and cable 4 have similar length at 90° and 270°. This is because the position of the EE is vertically symmetric. The EE was commanded to complete the tracing in 6 seconds. Fig. (b) and Fig. (c) show the EE cartesian velocity and joint velocity, respectively.

4. Experimental Setup and Process Parameters Design of Experiment

4.1. Representative Concrete Wall Specimen

A concrete wall to be grinded was represented by concrete samples with dimensions of 460mm x 460mm as shown in **Error!**

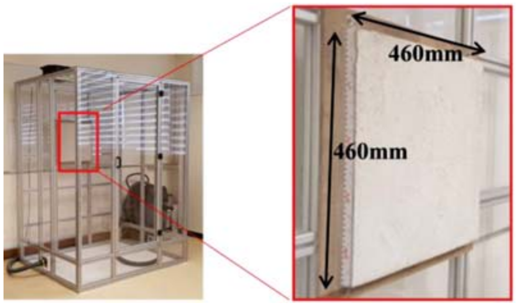

Fig. 4 Experimental test setup with concrete wall specimen

Reference source not found..

4.2. Polishing Frame

Polishing experiments were conducted using a handheld grinder (Makita PC5010C) with a vacuum shroud. The shroud was connected to an industrial vacuum cleaner to extract the dust. As the polishing force was affected by the negative pressure from the vacuum cleaner, a polishing frame was designed to control the contact force and limit the grinder from having excessive motion into the surface (see Fig. (a)). When the polishing force was not applied, there would be a 10mm distance between the grinding media and the wall surface (see Fig. 5(b)). By implementing a passive spring mechanism at the 4 frame legs, the grinding media would have contact on the specimen surface only when a polishing force was applied to the specimen surface. A 250N rated load cell was also embedded to monitor applied polishing force. The polishing path was conducted vertically (from top to bottom, see Fig. 5(c)), once per trial, while recording the polishing force with a data logger. A video of the trial was also recorded to facilitate in capturing the polishing linear speed. The vertical linear path was performed in order to obtain a consistent experimental condition.

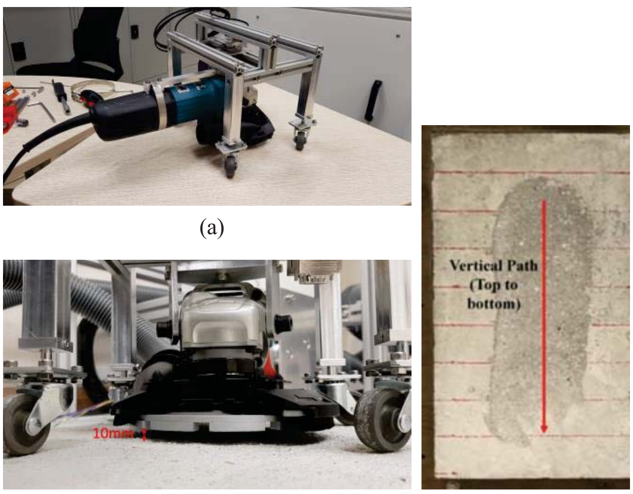

(a) (b) (c)

Fig. 5 (a) Polishing frame (b) There is a 10mm distance between the grinding media and the wall surface when force is not applied (c) Grinding trial path on concrete specimen

4.3. Design of Experiment

The Design of experiment (DOE) methodology was employed to evaluate the effects of input parameters on output parameters as well as to reduce the number of tests to be conducted [4], thereby enhancing the efficiency of the trials. DOE facilitates in finding suitable and dominant input variables in polishing process. In order to investigate the polishing process parameters, two levels (i.e., low and high) of input variables (i.e., grinder rotation speed and wheel media type) were investigated (see Table 1). The grinder's rotation speed was selected from the grinder's variable speed controller as shown in Fig. (a). The low-speed level is selected to be the minimum rotation speed of the grinder and the high-speed level is selected to be the maximum rotation speed of the grinder. As for the grinding wheel media, they were selected to be the single row and turbo types (see 6(b) and 6(c)), based on the recommendations provided by industry end-users involved in concrete wall grinding process. As there were only two input variables, a full factorial DOE was considered practical in this investigation. A full factorial DOE measured the response of every possible combination of input variables and their levels. There were a total of 2^n required number of experiments, where n is the number of input variables, which was 2 in this case, resulting in a total of 4 (=2^2)

Table 1 Low and high levels of input variables

Input variables	Low level (-1)	High level (1)
Polisher rotation speed (rpm)	4000	9000
Polisher wheel media type	Single Row	Turbo

(a) (b) (c)

Fig. 6 Grinder's variable speed controller and 5 inch Low-Vibration Diamond Cup Wheel (b) Single Row and (c) Turbo

Table 2 Design of experiment matrix and experimental results

	Input variables		Output variables		
No	Grinding rotation speed	Grinding wheel type	Average force (N)	Platform Speed (mm/s)	Roughness
1	-1	-1	37	18	Medium
2	1	-1	32	25	Smooth
3	-1	1	38	28	High
4	1	1	27	42	High

experiments to be conducted.

5. Results and Discussion

A total of 4 different permutations of experiments were conducted and with their corresponding output variable results (see Table 2). The polishing force was measured by a load cell embedded at the polishing frame, while the platform speed was analyzed from the line grids created on the specimen and recorded video (see Fig. 7). The surface roughness was determined via visual inspection and touching the surface. As shown in Table 2, that the average polishing force was determined to be 33N. As expected, the platform speed increased with the increase of the grinding rotation speed. The type of grinding media also affected the platform speed. The turbo media was observed to require a higher platform speed compared to the single row type. However, the roughness produced by the turbo type was rougher than the single row type. Fig. 8 shows the visual of the concrete wall surface roughness, before and after grinding. The investigation concluded with the recommendation of using the single row type of grinding media wheel, with a grinding speed of 9,000 rpm and approx. 30N of grinding force.

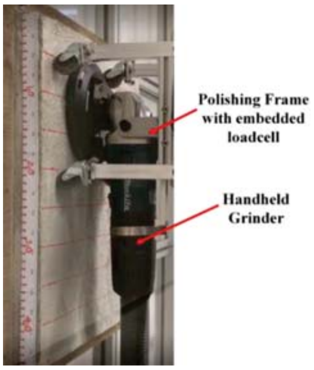

Fig. 7 Line grids on concrete specimen to aid in analyzing linear grinding speed

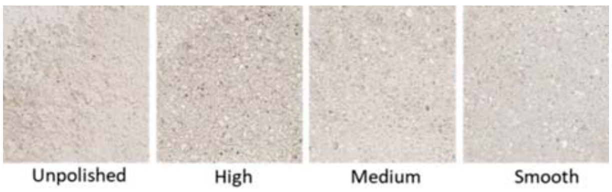

Fig. 8 Visual indication of surface roughness, before (unpolished) and after (high, medium, smooth) polishing

6. Conclusion

This paper presented the design of a three degrees-of-freedom planar, parallel robot, based on the cable-driven parallel mechanism design, with the key features of being modular, mobile and lightweight. One of the key enablers in transitioning from a manual to an automated grinding was the understanding of the appropriate grinding process parameters, in order to obtain an acceptable concrete surface finishing result. A full factorial design of experiment was conducted with preliminary results indicated that the grinding of common defects required a normal grinding force of approximately 30N, with a grinding speed of 9000 rpm and using the single-row diamond cup wheel as the grinding media.

ACKNOWLEDGEMENT

This work was supported by the ‘Robotics for Construction 4.0’ project (Grant ID: 1922200001), under A*STAR’s ‘National Robotics Programme – Robotics Domain Specific’ funding. The authors would also like to thank Mr How Woei Seng from the Professional Officers Division, Singapore Institute of Technology, for his insights shared during the experimental trials.

REFERENCES

1. VCP. Inc., "Vertical Concrete Polishing," 22 July 2022. [Online]. Available: https://www.verticalconcretepolishing.com/home. [Accessed 22 July 2022].
2. TP Tho, NT Thinh, "Using a Cable-Driven Parallel Robot with Applications in 3D Concrete Printing," Applied Sciences, vol. 11, no. MDPI AG, pp. 563, 2021.
3. RL Williams, P Gallina, "Planar cable-direct-driven robots, part I: Kinematics and statics," Proceedings of the ASME Design Engineering Technical Conference, vol. 2 American Society of Mechanical Engineers Digital Collection, pp. 1233–1240, 2001.
4. Giles, John R. Wagner and Eldridge M. Mount and Harold F., "25 - Design of Experiments," in Extrusion (Second Edition), William Andrew Publishing, 2014, pp. 291-308.